

Synthesis and characterisation of AlB₂ nanopowders by solid state reaction

Chunmei Jiang¹, Yongjun Ma^{1,2}, Fengqi Zhao³, Lun Wei³, Heng Zhang³, Chonghua Pei¹

¹State Key Laboratory Cultivation Base for Nonmetal Composites and Functional Materials, Southwest University of Science and Technology, Mianyang 621010, People's Republic of China

²Analytical and Testing Center, Southwest University of Science and Technology, Mianyang 621010, People's Republic of China

³Science and Technology on Combustion and Explosion Laboratory, Xi'an Modern Chemistry Research Institute, Shanxi 710065, People's Republic of China

E-mail: mayongjun@swust.edu.cn

Published in Micro & Nano Letters; Received on 12th November 2013; Accepted on 20th December 2013

A simple and effective way for preparing AlB₂ nanopowders was developed using solid state reaction with a mixture of nanometre-sized powders of aluminium and amorphous boron. The optimum synthesis conditions and the structural characteristics of the products were carefully investigated by means of X-ray diffraction, field emission scanning electron microscopy, transmission electron microscopy, high-resolution transmission electron microscopy and an energy dispersive spectrometer. The best result was obtained at a synthesis temperature of 900°C for 2 h with a molar ratio of 1:1.8. The obtained AlB₂ nanopowders consisted of numerous anomalous spherical particles with the grain size ranging from 100 to 200 nm. Furthermore, differential scanning calorimetry analysis showed that the combustion characteristics of the as-prepared AlB₂ nanopowders were better than that of the commercial AlB₂ powder under the same condition.

1. Introduction: Wide applications of AlB₂ in the fields of aluminium grain refiner, aluminium metal matrix composites, reaction partner in a hydrogen storage system and solid rocket propellant have made this metal boride the focus of many interesting projects [1–5]. Since its performance in these applications has a direct relationship with the properties of the powders and it is known that the nanometre materials generally possess many novel physical and chemical properties because of the small size effect, high surface effect and quantum size effect, therefore synthesis of the AlB₂ nanometre powders looks much more attractive from the application point of view [6, 7]. So far, there have been only two reports about preparation of the AlB₂ nanopowders. Fan *et al.* [8] obtained AlB₂ nanowires with lateral dimensions of about 200 nm and with lengths extending to more than a few micrometres by the reaction of the aluminium powders with BCl₃ gas on Si substrates using Ni(NO₃)₂ as catalysts. Ağaoğulları *et al.* [9] synthesised the AlB₂ nanopowders in sizes between 35 and 75 nm by using a combined method of mechanical alloying and annealing of elemental aluminium and boron powders. However, for the widespread use of the AlB₂ nanopowders in many fields, there is still a need to develop a simple, efficient and environmentally friendly method, because the existing methods generally have a complicated manufacturing process and are difficult to carry out in large-scale production.

It is well known that the solid state reaction is usually rapid, simple, free from pollution and can be easily industrialised. When the solid state synthesis takes place between the elemental reactants, it becomes easy to control the product composition. Therefore the objective of our Letter revolves around the feasibility and the practicality of producing AlB₂ nanopowders directly by integrating boron with aluminium. In this investigation, we chose nanometre aluminium and nanometre boron as the raw materials. One reason is that nanometre aluminium can be easily combined with the surrounding materials because of its high activity; nanometre boron is much easier for preparing boride with a smaller particle size distribution because the grain size of boron has a direct bearing on the grain size of the final products. The other reason is that the uniformity of the fabricated AlB₂ would be largely improved by using the nanometre-size raw materials. Special crucibles and suitable

working conditions were designed to obtain an oxygen-free environment.

Discussed in this Letter, the AlB₂ nanopowders were directly synthesised by a simple solid state reaction. Meanwhile, the optimum synthesis conditions and the structural characteristics of the products are fully characterised. The possible growth mechanisms and the excellent energetic performance of the AlB₂ nanopowders are also discussed.

2. Experimental

2.1. Materials: Aluminium powder (99.9% purity, 100 nm average particle size) was purchased from Aladdin Industrial Corporation, China. Amorphous boron powder (99.9% purity, 500 nm average particle size) was purchased from Shanghai ST-NANO Science&Technology Co., Ltd, China. Commercial AlB₂ powder was purchased from Shanghai Sigma-Aldrich Trade Co., Ltd, China. Alcohol (analytical reagent) was purchased from the Chengdu area of the industrial development zone Xindu Mulan, China.

2.2. Synthesis of the AlB₂ nanopowders: The method that was employed to synthesise the AlB₂ nanopowders was based on the combination reaction of Al with B and the detailed preparation process could be described as follows. Firstly, commercial aluminium powder and amorphous boron powder were mixed thoroughly with different molar ratios in proper absolute alcohol (analytical reagent) and then dried at 65°C for 12 h in a vacuum oven. Secondly, the obtained homogeneous mixtures were put into a small quartz ampoule (13 mm in diameter and 20 mm long) under an argon atmosphere in a glove-box. After the quartz ampoule was sealed, they were in turn sealed in a particular capsule and subsequently placed on the loading plate which was inserted horizontally in a quartz tube mounted inside the furnace. Thirdly, after the quartz tube had been evacuated to a base pressure of about 10 Pa by a mechanical rotary pump, an argon flow was introduced to fill the furnace, and this process was repeated three times to minimise the content of oxygen in the furnace. Subsequently, the samples were heated from room temperature to 750, 800, 850, 900 and 950°C, respectively, by using a 10°C/min heating ramp and held at this temperature

for 2 h while continually being pumped with a steady argon flow of 0.30 sccm. Finally, the quartz tube was cooled down to room temperature under a steady argon feed rate (0.20 sccm). A dark brown powder of AlB_2 nanopowder was taken out.

2.3. Characterisation: The X-ray diffraction (XRD) patterns were measured with a PANalytical X'Pert PRO Diffractometer by using $\text{Cu-K}\alpha$ radiation ($\lambda=0.154$ nm). SEM images were conducted on a field emission scanning electron microscope (ULTRA 55, ZEISS) operating at an accelerating voltage of 10 kV, equipped with an energy dispersive spectrometer (EDS). Transmission electron microscope (TEM) images were measured on a TEM combined with a high-resolution TEM (TEM/HRTEM, Libra 200FE, ZEISS) operated at 200 kV. Differential scanning calorimetry (DSC) was performed on an SDT Q600 thermal analyser with a heating rate of $20^\circ\text{C}/\text{min}$ from room temperature to 1200°C in air.

3. Results and discussions: To obtain an optimum synthesis, different Al/B molar ratios were selected, as shown in Fig. 1. When the sample was heated in a temperature of 850°C with a molar ratio of 1:2, the XRD pattern showed mainly AlB_2 and a small amount of Al_2O_3 . As the boron content decreased, the intensity of the AlB_2 diffraction peaks increased gradually, indicating a higher crystallinity. However, excessive Al began to emerge and increased gradually when the molar ratio was larger than 1:1.8. Five different sintering temperatures of 750, 800, 850, 900 and 950°C , for 2 h (Al/B = 1:1.8) were selected, as shown in Fig. 2. Each spectrum is labelled on the left side specifying the sintering temperature. From Fig. 2, we can see that the XRD pattern for Al+2B shows large aluminium peaks with a small amount of boron. Only when the temperature reached 750°C , a little AlB_2 was generated, and with the rise of temperature, its content increased. As the sintering temperature increased to 900°C , the diffraction peaks of the residual components gradually vanished, accompanied by the AlB_2 phase increasing and becoming the predominant phase. The characteristic peaks were located at $2\theta=27.4^\circ(001)$, $34.4^\circ(100)$, $44.5^\circ(101)$, $56.5^\circ(002)$, $61.7^\circ(110)$, $67.9^\circ(102)$, $68.7^\circ(111)$, $72.5^\circ(200)$, $79.2^\circ(201)$ and $88.5^\circ(112)$, respectively. Those observed peaks were roughly matched with the standard data of AlB_2 (JCPDS No.65-3381). At the same time, we could see that little Al_2O_3 impurities existed in all the temperature ranges. Partial decomposition of AlB_2 occurred and the formation of AlB_{12} and elemental Al were observed after heating at 950°C , which were consistent with the

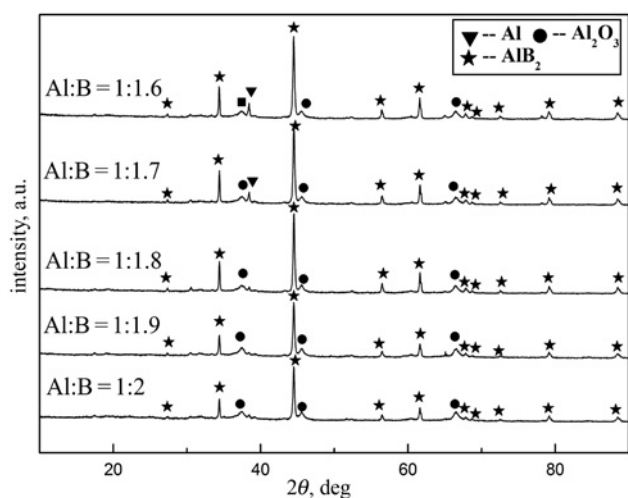


Figure 1 XRD patterns of the products synthesised with different Al/B mole ratio

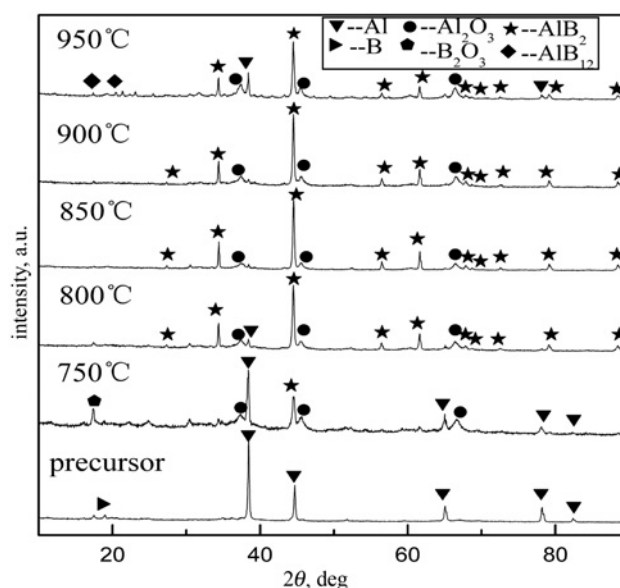


Figure 2 XRD patterns of the products synthesised at different sintering temperatures

phase diagram of the Al–B system [10, 11]. The experimental results of the presented work indicated that the optimum synthetic condition was at a temperature of 900°C for 2 h with a molar ratio of 1:1.8. Meanwhile, we found that the phase formation temperature of AlB_2 using nanometre raw material was almost the same as those of the sample prepared using the micron-sized raw materials reported previously [12]. However, the phase formation temperature of AlB_2 did not depend on the particle size of the raw Al and B powders.

Fig. 3a shows the plan-view of the SEM image revealing the general morphology of the AlB_2 nanopowders synthesised at 900°C for 2 h. It can be seen that the sample consisted of a lot of small particles and also appeared to have aggregation to some extent. The SEM image at high magnification indicated that the shape of the particles was anomalous spherical and the grain size ranged from 100 to 200 nm, as shown in Fig. 3b and c. What is

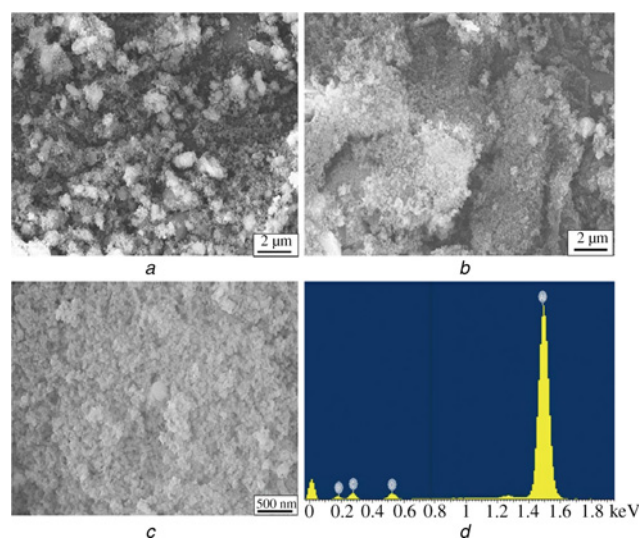


Figure 3 SEM and EDS images of the sample that synthesised at 900°C for 2 h

a Overall morphology of the products
b and c Enlarged images of the products
d EDS spectrum recorded from the as-prepared AlB_2 nanopowders

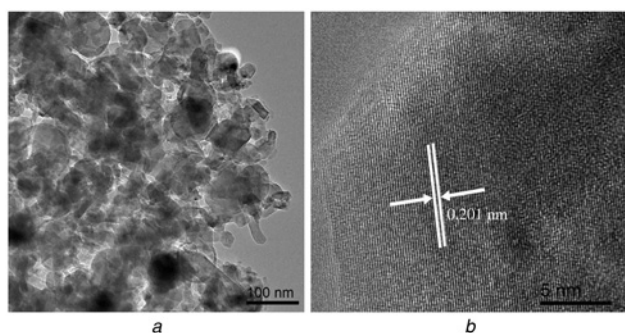


Figure 4 TEM and HRTEM images of the AlB_2 nanopowders synthesised at 900°C for 2 h
 a TEM
 b HRTEM

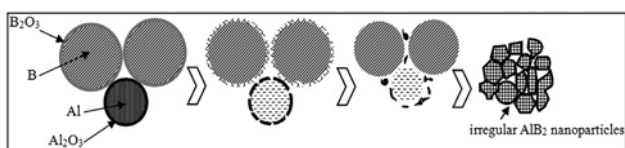


Figure 5 Schematic illustration of the growth mechanism

more, an EDS measurement was carried out to determine the chemical composition of the nanopowders. Fig. 3d is a qualitative EDS spectrum corresponding to an arbitrary nanoparticle. The same study was performed on many different nanoparticles and the results exhibited the presence of Al, B, C and O. The signal of carbon could be due to the contribution of porous carbon film for supporting samples and the appearance of oxygen might be derived from the oxidation of the raw material. It was difficult to detect the B component accurately because of the small atomic number of the light elements, and thus based on the analysis of the EDS spectrum, it was difficult to confirm the exact composition of the AlB_2 nanopowders.

To further study the morphologies, the growth properties and the lattice parameters of the products, TEM and HRTEM were employed. The results are shown in Fig. 4. According to the TEM image (Fig. 4a), it can be seen that most of the AlB_2 nanoparticles were quasi-spherical and their diameter was around 150 nm. Some agglomeration also took place which may be attributed to a large specific surface area and a high surface energy. This aggregation occurred probably during the process of cooling after sintering. Fig. 4b illustrates a HRTEM image of a single nanoparticle, which presented with clear lattice fringes and an interplanar spacing of around 0.201 nm, and this value corresponds roughly with the interplanar distance of the (101) crystal plane of AlB_2 .

Based on the above observations, we put forward a possible growth mechanism and a schematic illustration is presented in Fig. 5. Nanoaluminium and nanoboron powders might inevitably react with a little adventitious oxygen to form a thin oxide layer, although they had been stored under an argon atmosphere after delivery. As the temperature gradually increased, a fracture of the alumina shell occurred in the weakest place (near the defects) and propagated across the shell under the stress of the thermally expanding core [13–16] and at the same time, the B_2O_3 layer that coated on the surface of the nanoboron particles had melted and formed a viscous liquid [17–19]. Then, the alumina shell cracks created a type of channel that could make the liquid B_2O_3 react with the aluminium particle core [20]. In the presence of aluminium, B_2O_3 may be reduced by aluminium to form Al_2O_3 and therefore clean boron was gradually exposed. Owing to the relatively low levels of B_2O_3 and free oxygen in a sealed container, the alumina shell that had

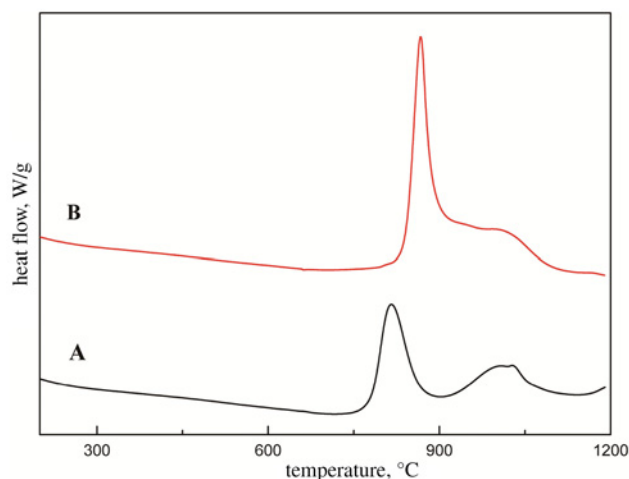


Figure 6 DSC curves of different AlB_2 powders
 A: commercial AlB_2 powder; and B: nanosized AlB_2 powder prepared by us

been healed would further crack with the increase of the temperature. The liquid Al that flowed through the gap had extremely high chemical reactivity, and thus, could quickly be combined with the surrounding exposed boron particles to form the so called irregular AlB_2 nanoparticles.

Fig. 6 shows the combustion performance of different AlB_2 powders in air. A was the commercial AlB_2 powder (about 2 μm) and B was the nanosized AlB_2 powder prepared by us. As can be seen from this Figure there existed big differences between them. Sharper and narrower exothermic peaks at the higher temperature were observed for the nanosized AlB_2 powder, and the combustion heat of the commercial AlB_2 powder was calculated to be of 9.297 kJ/g, whereas for the as-prepared AlB_2 nanopowders its value reached up to 21.019 kJ/g. These results indicated that the combustion characteristics of our nanosized AlB_2 powder were much better than that of the commercial product.

4. Conclusion: A simple and effective route for the synthesis of the AlB_2 nanopowders has been presented. The SEM and the TEM observations indicated that the as-prepared AlB_2 nanopowder had an anomalous spherical shape with the diameter ranging from 100 to 200 nm. Their formation process could be explained by the conventional diffusion growth mechanism. Compared with the commercial AlB_2 powders, the prepared AlB_2 nanopowders showed better combustion performance, in which the DSC exothermic peaks became narrower and sharper and the corresponding areas increased on a large scale. Besides, this presented work might provide a new insight into the synthesis of the other metal boride nanocrystalline particles.

5. Acknowledgments: This work was financially supported by grant no. (11zxzk26) from the Open Foundation of the State Key Laboratory Cultivation Base for Nonmetal Composites and Functional Materials, China and grant no. (9140C350202110C3501) from the Foundation of Science and Technology on Combustion and Explosion Laboratory, China.

6 References

- [1] Wang X.: 'The formation of AlB_2 in an Al–B master alloy', *J. Alloys Compd.*, 2005, **403**, pp. 283–287
- [2] Matkovich V.I., Economy J., Giese R.F.: 'Presence of carbon in aluminum borides', *J. Am. Chem. Soc.*, 1964, **86**, pp. 2337–2340
- [3] Deppisch C., Liu G., Shang J.K., Economy J.: 'Processing and mechanical properties of AlB_2 flake reinforced Al-alloy composites', *Mater. Sci. Eng. A*, 1997, **225**, pp. 153–161

- [4] Kang X.D., Wang P., Ma L.P., Cheng H.M.: 'Reversible hydrogen storage in LiBH_4 destabilized by milling with Al', *Appl. Phys. A*, 2007, **89**, pp. 963–966
- [5] Whittaker M.L.: 'Synthesis, characterization and energetic performance of metal boride compounds for insensitive energetic materials' (ProQuest LLC: University of Utah, 2012)
- [6] McCartney D.G.: 'Grain refining of aluminum and its alloys using inoculants', *Int. Mater. Rev.*, 1989, **34**, pp. 247–260
- [7] Saghatforoush L.A., Hasanzadeh M., Sanati S., Mehdizadeh R.: 'Ni $(\text{OH})_2$ and NiO nanostructures: synthesis, characterization and electrochemical performance', *Bull. Korean Chem. Soc.*, 2012, **33**, pp. 2613–2618
- [8] Fan Q.H., Zhao Y.M., Huang J., Ouyang L.S., Kuang Q.: 'Large-scale synthesis of aluminum diboride nanowires by Ni $(\text{NO}_3)_2$ catalyst', *J. Cryst. Growth*, 2012, **346**, pp. 75–78
- [9] Ağaoğulları D., Gökçe H., Duman İ., Öveçoğlu M.L.: 'Influences of metallic Co and mechanical alloying on the microstructural and mechanical properties of TiB_2 ceramics prepared via pressureless sintering', *J. Eur. Ceram. Soc.*, 2012, **32**, pp. 1949–1956
- [10] Fjellstedt J., Jarfors A.E., El-Benawy T.: 'Experimental investigation and thermodynamic assessment of the Al-rich side of the Al–B system', *Mater. Des.*, 2001, **22**, pp. 443–449
- [11] Duschaneck H., Rogl P.: 'The Al–B (aluminum–boron) system', *J. Phase Equilib.*, 1994, **15**, pp. 543–552
- [12] Felten E.J.: 'The preparation of aluminum diboride, AlB_{21} ', *J. Am. Chem. Soc.*, 1956, **78**, pp. 5977–5978
- [13] Levitas V.I., Asay B.W., Son S.F., Pantoya M.: 'Mechanochemical mechanism for fast reaction of metastable intermolecular composites based on dispersion of liquid metal', *J. Appl. Phys.*, 2007, **101**, pp. 083524–083524
- [14] Levitas V.I.: 'Strong effect of the heating rate and melt-dispersion mechanism', *Combust. Flame*, 2009, **156**, pp. 543–546
- [15] Firmansyah D.A., Sullivan K., Lee K.S., *ET AL.* 'Microstructural behavior of the alumina shell and aluminum core before and after melting of aluminum nanoparticles', *J. Phys. Chem. C*, 2011, **116**, pp. 404–411
- [16] Sun J., Simon S.L.: 'The melting behavior of aluminum nanoparticles', *Thermochim. Acta*, 2007, **463**, pp. 32–40
- [17] Young G., Sullivan K., Zachariah M.R., Yu K.: 'Combustion characteristics of boron nanoparticles', *Combust. Flame*, 2009, **156**, pp. 322–333
- [18] Chen C., Wang Y.H., PAN K.Z.: 'Thermal-characteristic research of boron', *J. Solid Rocket Technol.*, 2009, **6**, pp. 663–666.
- [19] Yeh C.L., Kuo K.K.: 'Ignition and combustion of boron particles', *Prog. Energy Combust. Sci.*, 1996, **22**, pp. 511–541
- [20] Whittaker M.L., Cutler R.A., Anderson P.E.: 'Boride-based materials for energetic applications', (MRS Proceedings, Cambridge University Press, USA, 2012)